

1  
2  
3  
4  
5  
6  
7  
8  
9  
10  
11  
12  
13  
14  
15

**Single Cell Chemical Proteomics (SCCP) Interrogates the Timing and Heterogeneity of  
Cancer Cell Commitment to Death**

Ákos Végvári\*, Jimmy E Rodriguez, Roman A Zubarev\*

Division of Physiological Chemistry I, Department of Medical Biochemistry & Biophysics,  
Karolinska Institutet, Biomedicum A9, Solnavägen 9, SE-171 77 Stockholm, Sweden

Contact to corresponding authors: [akos.vegvvari@ki.se](mailto:akos.vegvvari@ki.se) (phone: +46-8-524 877 07) and  
[roman.zubarev@ki.se](mailto:roman.zubarev@ki.se) (phone: +46-8-524 875 94)

16 **Abstract**

17 Chemical proteomics studies the effects of drugs upon cellular proteome. Due to the complexity  
18 and diversity of tumors, the response of cancer cells to drugs is also heterogeneous, and thus  
19 proteome analysis at single cell level is needed. So far, single cell proteomics techniques have  
20 not been quantitative enough to tackle the drug effects on the target proteins. Here, we  
21 developed the first single cell chemical proteomics (SCCP) technique and studied with it the  
22 time-resolved response to anticancer drugs methotrexate, camptothecin and tomudex of  
23 individual adenocarcinoma A549 cells. For each drug SCCP identified and quantified 1,000-  
24 2,000 proteins across >150 single cells in a time course of treatment up to 48 h, revealing the  
25 early emergence of cellular subpopulations committed and uncommitted to death. SCCP  
26 represents a novel approach to exploring the heterogeneous response to drugs of cancer cells.

27

28 **Keywords:** TMT labeling; Drug sensitivity; Resistance to drugs; Cell death; Methotrexate;  
29 Camptothecin; Tomudex

30

## 31 **1. Introduction**

32 Chemical proteomics studies the effects of drugs on cellular proteomes with the purpose of  
33 deciphering the targets and mechanisms of action (MOAs) of these molecules.<sup>1-3</sup> When  
34 sensitive cells are treated with toxic compounds for extended period of time, mechanistic target  
35 proteins become significantly regulated, and their profiling provides the first hint on the  
36 compound's targets and MOA.<sup>4,5</sup> This approach has been employed in functional identification  
37 of target by expression proteomics (FITExP)<sup>6</sup>, which laid ground for the online chemical  
38 proteomics ProTargetMiner tool.<sup>1</sup> In FITExP, cells are treated at a LC<sub>50</sub> concentration for 48 h,  
39 by which time half of the cells die. The dying cells detach from the substrate (for adherent cell  
40 types) and are found floating on the flask surface. In the remaining (surviving) cells, the drug  
41 target's expression level is significantly and specifically regulated up or down, which serves a  
42 basis for drug target identification in FITExP. As an example, when cancer cells undergo  
43 treatment with methotrexate (MTX), the target protein dihydrofolate reductase (DHFR)  
44 becomes highly upregulated before the cells undergo programmed cell death.<sup>7-9</sup> Interestingly,  
45 while the proteomes of the dying and surviving cells are very different (lending support to the  
46 notion that cell death is the ultimate case of cell differentiation), the drug target behaves in a  
47 similar manner in both types of cells.<sup>2</sup>

48 The adherent cells usually start losing their attachment to the surface after 24 h of  
49 treatment at LC<sub>50</sub> concentration, but the decision to survive or become dying must be made by  
50 the cell well before that.<sup>1,10,11</sup> The intricate details of this decision making process are of great  
51 scientific interest, as they possibly hold keys to drug resistance mechanisms.<sup>1,6</sup> These decision  
52 making processes can only be studied at the single cell level, while all so far reported chemical  
53 proteomics studies relied on bulk cell analysis.<sup>12</sup> Cellular heterogeneity is currently analyzed  
54 routinely by single cell transcriptomics (SCT),<sup>13</sup> with mRNA levels assumed to be proportional  
55 to the protein expression levels. However, at any given moment the concentration of both

56 mRNA and proteins reflects the balance between their corresponding expression and  
57 degradation, and while mRNA transcription and protein expression are linked together rather  
58 well, the degradation processes for mRNA and proteins are completely decoupled. As a result,  
59 in the biological processes driven mostly by protein expression, mRNA levels provide excellent  
60 proxy for protein concentrations, but this correlation seems to break down already at steady  
61 states of the cell.<sup>14</sup> In cell death processes mediated by protein degradation (*e.g.*, via caspase  
62 proteases), a correlation between mRNA and protein levels cannot be presumed. Therefore,  
63 cell heterogeneity in death-related processes can best be studied with single cell proteomics  
64 (SCP).

65 Compared to the rather well developed SCT approaches, SCP methods are still  
66 emerging. While some targeted antibody-based immunoassays have been applied to  
67 characterize proteins in single cells,<sup>15,16</sup> these approaches are limited to a few dozen proteins  
68 per experiment and exhibit strong bias in quantification. Mass spectrometry (MS)-based  
69 proteomics can in principle overcome these limitations, but lacking the benefit of PCR, MS  
70 proteomic analysis at a single cell level is very challenging due to the extremely low amounts  
71 of proteins (ca. 0.2 ng in a mammalian cell), the high dynamic range of protein expression (7  
72 orders of magnitude versus 3-4 orders for mRNAs),<sup>17,18</sup> and the inevitable sample loss during  
73 protein extraction, digestion and chromatographic separation of the peptide digest.<sup>19</sup>  
74 Consequently, despite the introduction of such ground-breaking SCP methods as SCoPE-MS<sup>19</sup>,  
75 SCoPE2<sup>20,21</sup> and nanoPOTS<sup>22</sup> that have been able to analyze between 500 and 2000 proteins in  
76 diverse cell lines, SCP has not been sufficiently quantitative to apply the techniques of chemical  
77 proteomics, such as FITExp. Thus, we have embarked on a painstaking enterprise of solving  
78 this issue to develop Single Cell Chemical Proteomics (SCCP).

79 Most SCP studies so far have considered two different types of cells (*e.g.*, monocytes  
80 vs macrophage cells or Jurkat vs U-937 cells)<sup>19,21</sup> with vastly different proteomes. Separation

81 of these cells by SCP was relatively straightforward as it could be done using a few most  
82 abundant proteins. In contrast, in cells influenced by a drug the most significantly regulated  
83 proteins (drug targets) are seldom highly abundant, being frequently found in the abundance-  
84 sorted list below the 1000<sup>th</sup> position. Therefore, our SCCP-development efforts were directed  
85 to achieving the following two intermediate objectives. First, average protein abundances in a  
86 homogeneous cell population measured by SCP must correlate with the abundances in bulk  
87 proteome analysis. This goal was achieved by starting from analyzing as bulk a relatively high  
88 number of cells and gradually reducing this number down to single cells, monitoring the  
89 correlation with the bulk analysis and systematically troubleshooting when this correlation  
90 broke down. A number of issues have been found and resolved related to protein extraction,  
91 digestion, labeling with isobaric reagents, LC separation, MS acquisition and statistical analysis.  
92 At the end, satisfactory correlations between SCP and bulk proteomics results were consistently  
93 obtained. The second intermediate goal objective was to detect with SCP the known strong  
94 regulation of the drug targets, as in FITeXP, with high statistical significance. This again  
95 required systematic studies and optimizations.

96 Here we present the developed SCCP workflow applied to studying in a time-course  
97 manner the proteome effects of anticancer drugs MTX, camptothecin (CPT) and tomudex  
98 (TDX), also known as raltitrexed. These drugs were applied at LC<sub>50</sub> concentration to A549  
99 human lung adenocarcinoma cells, leading half of the cells to death in 48 h. Our workflow  
100 comprises the isolation of cells using fluorescence-activated cell sorting (FACS), minimal  
101 sample preparation including tryptic digestion, tandem mass tag (TMT) isobaric labeling for  
102 protein quantification, incorporation of a carrier proteome (CP) to boost the MS signal,  
103 chromatographic separation at a low flow rate, MS/MS data acquisitions and SCCP-optimized  
104 data processing (see **Figure 1**). The goal of the study was to identify the time scale of the  
105 decision-making dying/surviving process, *i.e.*, to reveal at what time the homogeneous cell

106 population started to differentiate under the influence of a drug into cells committed to  
107 surviving or dying.

## 108 109 **2. Results**

### 110 **2.1. Improving critical steps of the SCCP workflow**

111 To establish a robust analytical method, a human lung cancer cell line A549 was selected as a  
112 cellular model because of its easy cultivation and handling. The cell size (ca. 10  $\mu\text{m}$  in diameter)  
113 permitted isolation of single cells by FACS without using surface markers for gating. The cells  
114 treated with MTX ( $\text{LC}_{50} = 1.15 \mu\text{M}$ ), CPT ( $\text{LC}_{50} = 3 \mu\text{M}$ ), TDX ( $\text{LC}_{50} = 50 \mu\text{M}$ ) and vehicle  
115 (DMSO) exhibited in FACS homogeneous populations that only changed shape when drug was  
116 applied (**Figure S1**). We consider FACS homogeneity (single population) an important element  
117 of any SCP study that justifies single cell analysis, as otherwise cell subpopulations can be  
118 counted, isolated by FACS and conventionally analyzed as bulk.

119 All drugs were known to strongly regulate their targets after 48 h incubation in A549  
120 cells.<sup>1</sup> Since cell lines are known to “drift” with time, we corroborated the regulation of DHFR,  
121 topoisomerase 1 (TOP1) and thymidylate synthase (TYMS) as the targets of MTX, CPT and  
122 TDX, respectively, in our cellular model using bulk proteome analysis.

123 The sample preparation optimization started from the SCoPE-MS strategy with  
124 TMT10plex labeling and 200 cells in the CP channel,<sup>19</sup> and was adapted to maximize the  
125 number of detected proteins and the precision of their quantification. Among the optimized  
126 parameters was the volume of buffer to capture cells on plate. Smaller volumes give higher  
127 protein concentration but are more difficult to handle, which potentially leads to larger losses.  
128 The results were comparable for volumes in the 1-5  $\mu\text{L}$  range (16,000-20,000 peptides and  
129 2200-2400 proteins quantified), and for practical reasons 5  $\mu\text{L}$  was chosen for all subsequent  
130 experiments.

131 We found that the property of the ABIRD device to significantly (2-3 times) reduce the  
132 chemical noise was especially beneficial in SCP, and utilized this device in all experiments.  
133 The flow rate across the EASY-Spray™ C18 analytical columns was reduced from the nominal  
134 ~300 nL/min to 100 nL/min to increase the signal abundance. Further reduction in the flow rate  
135 reflected negatively on spray stability. We also increased the accumulation time in the Orbitrap  
136 for MS/MS above the recommended maximum 86 ms to 150 ms. These measures allowed us  
137 to identify and quantify over 2000 proteins in a stable way across 64 cells.

138 Significant improvements were required in data analysis. PCA of raw SCP data gave no  
139 separation between the treated and untreated cells; the data clustered instead according to the  
140 TMT sets. To address this inherent for SCP batch effect, we employed the batch-compensation  
141 function in the *SVA* package using empirical Bayesian approach. We also found that it was  
142 important to normalize the peptide and protein abundances by the median abundance in a given  
143 cell. Using these approaches, we started to obtain treated-untreated group separation in PCA.

144

## 145 **2.2. Introducing split semi-bulk CP**

146 In order to verify that the separation between the cell groups in PCA was related to biology  
147 and was not an uncompensated artefact, we introduced a CP in two separate channels. In  
148 general, CP channel is commonly used in TMT-SCP to increase the identification rate and  
149 reduce the risk of a catastrophic sample loss during sample preparation.<sup>19,23,24</sup> Most often, 200  
150 cells or their equivalent are used for CP, and since its effect on ion signal is additive<sup>25</sup>, we split  
151 the CP between two channels, with one channel carrying 100 treated cells and another one –  
152 100 untreated cells. The expectation was that the average (or median) protein abundances in  
153 single treated cells will correlate with the protein abundances in treated CP, and the untreated  
154 cells will correlate with untreated CP.

155 Failure to observe such correlation between single cell and bulk proteome data in our first  
156 such experiments made us reconsider the way how bulk proteome is obtained. In previous  
157 experiments, the bulk proteomic analysis was performed in a conventional proteomics way with  
158 the use of detergents, S-S bond reducing and alkylating agents, *etc.*, which significantly differed  
159 from SCP sample preparation. Then we prepared CPs the same way as single cell proteomes,  
160 calling such CPs semi-bulk. We used semi-bulk CPs for analysis of 84 MTX-treated and 84  
161 vehicle-treated single cells in 24 TMT11plex sets. Each of these sets these sets carried 7 single  
162 cells (3 or 4 for each condition), an untreated semi-bulk CP in the channel 131C and MTX-  
163 treated semi-bulk CP in the channel 131N, while two channels (130N and 130C) remained  
164 empty. In total, 13,142 peptides were quantified belonging to 1825 proteins. A satisfactory  
165 correlation ( $R=0.64$ ) was obtained between the  $\log_2$  values of the protein treated-control  
166 regulations in the semi-bulk CPs and the median SC data (**Figure 2A**), which was similar to  
167 the correlation between the semi-bulk CPs and the bulk-analyzed CPs prepared in the SCP  
168 manner from large number of cells ( $R=0.81$ , data not shown). In an OPLS-DA model where  
169 treated CP, control CP, treated single cell and untreated single cell data were pooled in four  
170 respective groups, single cell data clustered together with their corresponding CPs (data not  
171 shown). When only the top 25, 200, 900 most abundant proteins as well as all 1825 proteins  
172 were used for OPLS-DA, the  $Q^2$  quality coefficient increased with the number of proteins,  
173 proving that RIAs from most proteins in single cells were responsible for the observed  
174 separation and not just a few abundant molecules. This was an encouraging message for SCCP,  
175 as in Chemical proteomics most drug targets have medium abundance.

176 Importantly, the SCCP dataset contained the MTX target DHFR that was found on the 6<sup>th</sup>  
177 position from the top among the most significantly upregulated proteins (**Figure 2B**). These  
178 results gave us confidence that the SCP data can be used in Chemical proteomics for drug target  
179 determination and monitoring. In subsequent experiments we continued to use for carrier and



180 bulk proteomes the SCP protocol – that is, all subsequent CPs and bulk proteomes are “semi-  
181 bulk”. Also, in subsequent experiments we obtained CPs by sorting 100 or 200 cells into one  
182 well, thus ensuring that CP cells undergo the same FACS treatment as single cells.

183

### 184 **2.3. TMTpro™ in SCCP workflow**

185 The recently introduced 16-plex TMTpro™ offers the obvious advantage of multiplexing more  
186 single cells into one TMT set (12 vs. 7 in TMT11plex™). However, this advantage might come  
187 with a price paid in form of a lower single cell reporter ion signal in MS/MS, as it is distributed  
188 over larger number of channels. To test whether the trade-off is acceptable for SCCP, we  
189 analyzed 96 single A549 cells treated with MTX and 96 vehicle-treated cells with split CPs (in  
190 channels 126 and 127N) and obtained somewhat lower number of protein IDs but still  
191 comparable with the TMT11plex™ analysis. In total, 1515 proteins were TMTpro-quantified  
192 with 8870 peptides in single cells with 133 significantly regulated proteins, and 1874 proteins  
193 with 12,317 peptides in the CPs with 326 regulated proteins. The correlation between SC data  
194 and CPs was satisfactory ( $R=0.71$ ), and significant up-regulation of DHFR was also detected  
195 for both SCs and CPs. This result confirmed that SCP can be performed using the TMTpro  
196 labelling, but as 11-plex TMT provided somewhat deeper proteome coverage, we continued to  
197 use it for SCCP purposes. To accommodate more single cells in one TMT11plex set, for single  
198 cell analysis subsequently we used one CP (unless specified otherwise), composed of a 1:1  
199 mixture of treated and untreated cells, while separately analyzing these proteomes for  
200 calculating the correlation with single cell data.

201

### 202 **2.4. Time-course SCCP analysis**

203 The goal of the experiment was to determine the time point at which the attached cells make  
204 the decision to die, so that their proteome becomes altered to resemble that of the end-point  
205 detached (dying) cells rather than the end-point attached (surviving) cells. For that purpose, the

206 cells were treated with MTX for 3, 6, 12, 24 and 48 h at LC<sub>50</sub> concentration. The attached cells  
207 at each time point and the detached cells at 48 h were collected, and FACS-isolated 96 cells of  
208 each type were analyzed with SCCP using a single CP representing a mixture of the 48 h  
209 attached and 48 h detached cells. The bulk proteomes of 48 h detached and attached treated  
210 cells were analyzed separately. On average, over 1500 proteins and 10,000 peptides were  
211 identified and quantified in single cells at each incubation time. **Figure 3** shows how the  
212 attached treated and untreated cell populations, being almost indistinguishable on a PCA plot  
213 at 3 h treatment, become gradually separated with time, achieving nearly full separation at 12  
214 h.

215 In order to identify at each timepoint the cell subgroup that was committed to death and the one  
216 committed to survival in the attached treated population, a hierarchical cluster analysis of  
217 protein abundances was performed (**Figure S2**). It was assumed that the two most abundant  
218 cell clusters represent the subgroups of the future surviving and dying cell. The hypothesis was  
219 that, being put on a PCA plot together with the 48 h attached and detached cells representing  
220 the two ultimate cell destinies, the two subgroups will reveal their identities by being closer to  
221 the respective destiny type. For time points earlier than the commitment event, cell clustering  
222 into the two subgroups will be random, and thus both subgroups would end up in the middle of  
223 the OPLS-DA plot close to each other.

224 Both these predictions were confirmed when the median abundances of all 1170 quantified  
225 proteins and 100 most abundant proteins in group 1 (G1) and group 2 (G2) separated by  
226 clustering analysis of attached cells were used for building an OPLS-DA model. The model  
227 also included the data on 48 h attached cells and 48 h detached cells, which represented the  
228 final destinations of the survival and dying subpopulations (**Figure 4A**). For 3 h and 6 h  
229 treatments, there was an overlap of the dots representing the G1 and G2 clusters, with a  
230 separation between them in the direction of the destiny points at 12 h and longer treatment

231 times. G1 was thus acquiring a proteome profile corresponding to the dying fate, while G2  
232 represented the surviving subpopulation. As expected, the OPLS-DA separation between these  
233 two subpopulations grew with time. Similarly, the number of proteins with significantly  
234 changed abundances between the vehicle- and MTX-treated populations increased with time  
235 from 32 and 15 proteins at 3 and 6 h to 38, 121 and 134 proteins at 12, 24 and 48 h, respectively.  
236 Therefore, the A549 cell commitment to death occurs between 6 and 12 h past MTX treatment.  
237 This time scale is consistent with the earlier reports on dynamic proteomics measurements in  
238 cells treated with a drug at  $LC_{50}$  – in the first hours past treatment, the cells try to overcome the  
239 encountered difficulty, activating survival pathways, and only commit to death after such an  
240 attempt fails.<sup>1</sup>

241 Interestingly, at 12 h more separation was seen for the whole proteome, while at 24 h the 100  
242 most abundant proteins showed bigger separation. This observation agreed well with the notion  
243 that the cell path to death starts with the inner mechanism altering lower-abundant mechanistic  
244 proteins first, followed by the altering household proteins that change cell morphology.  
245 Consistent with this scenario, when the main OPLS-DA coordinates of the individual cells were  
246 plotted on a scale normalized such that the attached cells treated for 48 h had  $x = 1$  and the  
247 corresponding detached cells had  $x = -1$ , the obtained distributions of G1 and G2 cells were  
248 separated in 12 h for the full proteome, but less so for 400 most abundant proteins and not at  
249 all for top 100 proteins (**Figure 4B**). At the same time, for 24 h treatment the G1 and G2  
250 proteomes gave broad distributions separated more for highly abundant proteins, suggesting  
251 that cell morphology alteration is well underway.

252 Pathway analysis of 179 proteins with significantly different abundances in G1 versus G2 at 12  
253 h past MTX treatment revealed that they preferentially belong to metabolic, carbon metabolism,  
254 ribosome- and proteasome-related pathways (**Figure S3**).

255

## 256 **2.5. SCCP with camptothecin (CPT) and tomudex/raltitrexed (TDX)**

257 Similar results as with MTX were obtained with CPT and TDX, with the targets TOP1  
258 (downregulated) and TYMS (upregulated) emerging among the top proteins in the respective  
259 areas of the volcano plot (**Figure 5**). While these drugs have different MOAs and targets, the  
260 A549 cells have clearly formed two well separated clusters in PCA.

261

## 262 **2.6. Target percolation by OPLS-DA of MTX, CPT and TDX data**

263 The ultimate goal of a Chemical proteomics experiment is drug target identification, which can  
264 be obtained by contrasting a specific treatment against all other treatments and controls. While  
265 designing ProTargetMiner<sup>2</sup>, we found that on average it takes 30-50 contrasting treatments to  
266 identify (“percolate”) the target uniquely among thousands of proteins in the proteome as the  
267 most specifically up- or down-regulated protein. Here, we merged the MTX, CPT and TDX  
268 SCCP data (treatment vs. untreated control) at 48 h of treatment and contrasted one drug against  
269 the other two (**Figure S4**). For MTX, the target DHFR was 4<sup>th</sup> most specifically upregulated  
270 protein; for CPT, TOP1 was 15<sup>th</sup> most specifically downregulated protein; and for TDX, TYMS  
271 was 10<sup>th</sup> most specifically upregulated protein. These results demonstrate that SCCP has the  
272 potential for unique drug target identification, provided enough contrasting treatments are  
273 obtained.

274

## 275 **3. Discussion**

276

277 Considering that cell to cell heterogeneity is a fundamental property of highly complex cellular  
278 systems<sup>16</sup>, the analysis of proteomes at a single cell level is essential for understanding the  
279 complex diseases, such as cancer, where diverse phenotypes contribute to the survival and  
280 progression,<sup>26</sup> as well as for studying the mechanisms of cell resistance to anticancer treatment.

281 Here we demonstrated that SCP can be sufficiently quantitative for enabling Chemical  
282 proteomics approaches for drug target identification and monitoring. One important milestone  
283 was to achieve significant correlation between the average protein regulation factors in SCCP  
284 between the treated and untreated cells with those obtained with conventional bulk proteomics  
285 of these cells. Another important milestone was to demonstrate similar behavior of the drug  
286 target proteins in SCCP as in bulk Chemical proteomics. Finally, the possibility to “percolate”  
287 by a contrasting OPLS-DA analysis the drug targets has a paramount importance for the use of  
288 such a powerful drug target deconvolution method as ProTargetMiner.

289 While these achievements were the SCCP proofs of principle, time course analysis provided  
290 new biologically relevant information, confirming that cell commitment to death can now be  
291 studied at a proteome level for individual cells. Between 6 h and 12 h past treatment, a large  
292 group of attached drug-treated cells already committed to detach and form a floating dying  
293 population. Importantly, these changes were detected among the lower-abundant proteins,  
294 while highly abundant proteins remained at that point unaffected. It was even possible to  
295 determine the pathways and parts of cell machinery participating in the decision-making  
296 process.

297

#### 298 **4. Conclusions**

299 After the quantitative aspect of single cell proteomics has been improved, chemical proteomics  
300 at the level of single cells became reality. The detailed profiling with SSCP of the heterogeneity  
301 of cancer cell response to drugs or treatments and the mechanistic analysis with cellular  
302 resolution of resistance to therapy is now possible. Moreover, the FITeXP method of chemical  
303 proteomics is now applicable to single cells. The remaining challenges are however vast. For  
304 example, SCCP needs to provide deeper proteome analysis, targeting the benchmark of 5,000  
305 proteins quantified with  $\geq 2$  peptides. A great achievement would be if complementary tools of

306 chemical proteomics, such as proteome-wide integral solubility alteration (PISA) assay<sup>27</sup> could  
307 be implemented for single cells. With PISA, one could monitor the protein target engagement  
308 of the drug molecule. This, however, requires significant efforts in improving the methods of  
309 handling and analyzing ultra-small protein amounts.

310

311

## 312 **5. Methods**

### 313 **5.1. Cell culturing treatment**

314 Human A549 lung adenocarcinoma cells obtained from ATCC (Manassas VA) were grown in  
315 Dulbecco's Modified Eagle's Medium (DMEM – Lonza, Wakersville MD) supplemented with  
316 10% FBS superior (Biochrom, Berlin, Germany), 2 mM L-glutamine (Lonza) and 100 U/mL  
317 penicillin/streptomycin (Thermo, Waltham MA) at 37°C in 5% CO<sub>2</sub>.

318 The LC<sub>50</sub> values for the drugs (MTX, CPT and TDX) were determined by CellTiter-Blue<sup>®</sup> cell  
319 viability assay (Promega). Cells were seeded into 96 plates at a density of 3000 cells per well,  
320 and after 24 h of culture they were treated with serial concentrations of the respective drug:  
321 MTX (0 – 100 µM), CPT (0 – 100 µM) and TDX (0 – 100 µM). After 48 h, the media were  
322 discarded and replaced with 100 µL of fresh culture media. In each well, 20 µL of resazurin  
323 (CellTiter-Blue<sup>®</sup> Cell Viability Assay kit – Promega) were added to perform the viability assay.  
324 After 4 h of incubation at 37°C, fluorescence of wells was measured in Infinite F200 Pro  
325 fluorometer (Tecan) by detecting the ratio between the excitation at 560 nm and emission at  
326 590 nm. The LC<sub>50</sub> values were determined from the dose-response curves by calculating the  
327 concentration causing the 50% fluorescence reduction compared with the untreated control.

328 Cells were then cultured and treated with MTX, CPT and TDX at LC<sub>50</sub> concentrations in 75  
329 cm<sup>2</sup> flasks for 3, 6, 12, 24 and 48 h (for CPT and TDX only 12, 24 and 48 h treatment were  
330 performed). Control cells were treated with the vehicle (10 mM dimethyl sulfoxide - DMSO).

331 After each incubation time point, the supernatant was collected and the attached cells were  
332 disconnected from the surface with TrypLE (Gibco) for 5 min, after which they were harvested  
333 by centrifugation at 1000 rpm for 3 min. Both types of cells (detached and adhered) were  
334 washed twice with cold 1X phosphate buffered saline (PBS).

335

## 336 **5.2. Isolation of single cells by FACS**

337 Collected attached cells were subjected to FACS analysis in FACS Aria™ Fusion (BD  
338 Biosciences), in which cells were sorted based on the forward and side scatter  
339 (FSC/SSC) parameters only. Individual singlet cells were collected in a 96-well Lo-Bind plate  
340 (Eppendorf, Hamburg, Germany) containing 5 µL of 100 mM triethylammonium bicarbonate  
341 (TEAB) per well. A total of 96 single cells were sorted for each condition/drug (untreated and  
342 treated cells) using separate plates. In addition, a third plate was prepared, being dedicated only  
343 to CP. On that plate, 200 cells (100 treated plus 100 control) were collected per well in the first  
344 two rows. Altogether, 24 wells of CP cells were collected for each treatment and time point.

345

## 346 **5.3. Protein extraction and digestion**

347 Proteins from single cells and CPs were extracted in four freeze – thaw cycles. Plates were  
348 frozen for 2 min in liquid nitrogen and immediately heated at 37°C for 2 min. Proteins were  
349 denatured by heating the plates at 90°C for 5 min. The resulted protein solutions were  
350 centrifuged at 1000 rpm for 2 min to spin down all the volume present in the wells. Finally, 1  
351 µL of 25 ng/µL sequencing grade trypsin (Promega, Madison WA) in 100 mM TEAB was  
352 dispensed using a MANTIS® automatic dispenser (Formulatrix, Bedford MA). In the case of  
353 CP, digestion was achieved with 2 µL of trypsin solution added. Plates were incubated at 37°C  
354 overnight (16 h).

355

356 **5.4. TMT labeling**

357 Both TMT10plex™ (or TMT11plex™ including channel 131C) and 16-channel TMTpro™  
358 (ThermoFisher Scientific, Rockford IL) were used in this study. Unless specified, each  
359 TMT10plex™ set contained 4 control cells and 4 treated cells with tags interspaced, as well as  
360 a single channel with CP (200 cells in channel 131). TMT 130N was not used because of the  
361 cross contamination with the CP channel. Peptides were TMT-labeled by dispensing 1 µL of  
362 the respective TMT reagent dissolved in dry acetonitrile (ACN) at a concentration of 10 µg/µL  
363 using the MANTIS robot. Plates were incubated at room temperature (RT) for 2 h and then the  
364 reaction was quenched by adding 1 µL of 5% hydroxylamine (also with automatic liquid  
365 handler), following incubation at RT for 15 min. In the case of TMTpro™ labeling, each set  
366 contained 6 control cells and 6 treated cells with the tags interspaced. The CP was split in two  
367 channels, 126 and 127N, one composed of 100 control cells and the other one 100 treated cells.  
368 Channels 127C and 128N were left empty to prevent cross-contamination from CP channels.  
369 The labeled samples were pooled together using a 10-µL glass syringe (VWR, Japan), starting  
370 always with the CP samples in each TMT set in order to minimize sample loss during the  
371 pooling.<sup>19</sup> Samples were pooled into MS-sample vials with glass insert (TPX snap ring vial  
372 from Genetec, Sweden) and dried in a speed vacuum concentrator (Concentrator Plus,  
373 Eppendorf). Dry peptides were resuspended in 7 µL of 2% ACN, 0.1% formic acid (FA) prior  
374 to LC-MS/MS analysis.

375

376 **5.5. Bulk proteome analysis**

377 Unless specified,  $1 \times 10^6$  were harvested and washed twice with PBS. To each cell pellet, 150  
378 µL of 8M urea in 50 mM ammonium bicarbonate (AmBic) pH 8.5 were added, tubes were  
379 sonicated in bath at 4°C for 5 min and probe-sonicated for 40 s with a Vibra-cell™ ultrasonic  
380 liquid processor (VCX 130, Sonics & Materials Inc., Newtown CT) using pulse 2/2 with amp



381 20. Each cell lysate was transferred to a new tube, while the original tube was washed with 150  
382  $\mu\text{L}$  of 50 mM AmBic pH 8.5 and the wash was added to the new tube. Samples were centrifuged  
383 for 10 min at 13,000 g and 4°C. Protein concentration was measured with BCA protein assay.  
384 Proteins were reduced by adding 20 mM dithiothreitol in 50 mM AmBic and incubated at 37°C  
385 for 1 h, followed by alkylation with 40 mM iodoacetamide at RT for 30 min in the dark. Finally,  
386 proteins were digested by adding trypsin in a 1:50 ratio and incubating overnight at 37°C. The  
387 resulting peptides were cleaned-up on HyperSep™ filter plate (ThermoFisher Scientific,  
388 Rockford IL) then dried in a speed vacuum concentrator. Dried samples were dissolved in 100  
389 mM TEAB and labeled with TMT10plex™ reagents that were dissolved in dry ACN and then  
390 mixed with the peptide solutions and incubated at RT for 1 h. The reaction was quenched by  
391 adding 11  $\mu\text{L}$  of 5% hydroxylamine and incubating at RT for 15 min. Finally, samples with  
392 different TMT labels were pooled into a single tube, cleaned-up on HyperSep™ filter plate and  
393 dried in a speed vacuum concentrator prior to LC-MS/MS analysis.

394

## 395 5.6. RPLC-MS/MS analysis

396 Peptide samples were separated on a Thermo Scientific™ Ultimate™ 3000 UHPLC  
397 (ThermoFisher Scientific) using a 10 min loading at 3  $\mu\text{L}/\text{min}$  flow rate to a trap column  
398 (Acclaim™ PepMap™ 100, 2 cm x 75  $\mu\text{m}$ , 3  $\mu\text{m}$ , 100 Å - ThermoFisher Scientific). The  
399 separation was performed on an EASY-Spray™ C18 analytical column (25 cm x 75  $\mu\text{m}$ , 1.9  
400  $\mu\text{m}$ , 300 Å – ES802A, ThermoFisher Scientific). A constant flow rate of 100 nL/min was  
401 applied during sample separation achieved in a linear gradient ramped from 5%B to 27%B over  
402 120 min, with solvents A and B being 2% ACN in 0.1% FA and 98% ACN in 0.1% FA,  
403 respectively. LC-MS/MS data were acquired on an Orbitrap Fusion™ Lumos™ Tribrid™ mass  
404 spectrometer (ThermoFisher Scientific, San José CA), using nano-electrospray ionization in  
405 positive ion mode at a spray voltage of 1.9 kV. To reduce atmospheric background and enhance

406 the peptide signal-to-noise ratio, an Active Background Ion Reduction Device (ABIRD - ESI  
407 Source Solutions, LLC, Woburn MA) was used on the nanospray ion source. Data dependent  
408 acquisition (DDA) mode parameters were set as follows: isolation of top 20 precursors in full  
409 mass spectra at 120,000 mass resolution in the  $m/z$  range of 375 – 1500, maximum allowed  
410 injection time (IT) of 100 ms, dynamic exclusion of 10 ppm for 45 s, MS2 isolation width of  
411 0.7 Th with higher-energy collision dissociation (HCD) of 35% at resolution of 50,000 and  
412 maximum IT of 150 ms in a single microscan. The mass spectrometry proteomics data are  
413 deposited to the ProteomeXchange Consortium via the PRIDE partner repository<sup>28</sup> with the  
414 data set identifier PXD025481.

415

## 416 **5.7. Data analysis**

417 Raw data from LC-MS/MS were analyzed on Proteome Discoverer v2.4 (ThermoFisher  
418 Scientific), searching proteins against SwissProt human database (release July 30, 2019 with  
419 20,373 entries) and known contaminants with Mascot Server v2.5.1 (MatrixScience Ltd, UK)  
420 allowing for up to two missed cleavages. Mass tolerance for precursor and fragment ions was  
421 10 ppm and 0.05 Da, respectively. Oxidation of methionine, deamidation of asparagine and  
422 glutamine, as well as TMTpro or TMT6plex lysine and N-termini were set as variable  
423 modifications. Percolator node<sup>29</sup> in Proteome Discoverer was set to target false discovery rate  
424 (FDR) at 1% with validation based on  $q$ -value.

425 The TMT reporter ion abundances (RIA) at a peptide level were extracted from the search  
426 results. The subsequent analyses were performed in the RStudio (version 1.3.1073)  
427 programming language environment, the software for multivariate data analytics SIMCA (v.  
428 15.0.2.5959, Sartorius) and Perseus software platform.<sup>30</sup> Peptides from single cells with RIAs  
429 exceeding 10% of the abundance values for the respective carrier channel were filtered out,  
430 being considered a result of co-isolation or other interferences, resulting in about 30% of the

431 peptides discarded for further analysis. After filtering, the remaining RIAs were arranged into  
432 a matrix of peptide IDs (rows) vs. single cells (columns). All RIAs were log<sub>2</sub>-transformed and  
433 the data were normalized in columns by subtracting their median values computed, ignoring  
434 the missing values. Peptides quantified in less than ten cells were discarded (usually <0.05%  
435 peptides per dataset). Protein-level quantification was achieved by attributing each unique  
436 peptide to its respective top ranked protein within a protein group. As protein relative  
437 abundance, the median RIA value among the peptides belonging to that protein was taken. The  
438 new relative abundance matrix (protein IDs vs. single cells) was again normalized by  
439 calculating the median value for each column (or single cell), and then, subtracting the median  
440 value calculated to each abundance on the respective column. Missing values in the resulting  
441 matrix were imputed based on the normal distribution of valid values (method available in  
442 Perseus software platform<sup>31</sup>), using a width of 0.3 standard deviations of the Gaussian  
443 distribution of the valid values and a downshift of 1.8 standard deviations. Finally, the batch  
444 effects across the TMT sets were corrected by applying an empirical Bayesian framework in  
445 the SVA package<sup>32</sup>.

446 The obtained matrix of relative protein abundances was used for statistical analysis. Principal  
447 component analysis (PCA) was performed to determine the separation degree between the  
448 control and drug-treated cells and to identify the outliers (single cells outside the limits of the  
449 PCA diagram with  $p < 0.05$ ), which were removed from subsequent analysis. Resulting data  
450 were analyzed by orthogonal partial least squares discriminant analysis (OPLS-DA) and  
451 clustering analysis, and the fold changes were presented as volcano plots.

452

453

454

455

456 **6. Acknowledgements**

457 We would like to express our gratitude to Bogdan Budnik (Harvard Center for Mass  
458 Spectrometry, Harvard University, Cambridge MA) for discussion and advice on experimental  
459 design and suggesting the Mantis liquid handling robot, John Neveu (ESI Source Solutions,  
460 Woborn MA) and Erik Verschuuren (MS Wil B.V., Aarle-Rixtel, The Neatherlands) for  
461 ABIRD connection; Ujjwal Neogi and Flora Mikeloff (Karolinska Institutet) for valuable help  
462 with R algorithms, Indira Pla (Lund University) for useful advices in statistics and R algorithms,  
463 Willy Björklund, Erik Damgård and many others at Thermo Scientific for valuable technical  
464 support. The study was funded by the Swedish Research Council (grant 2018-06156, VR).

465

466 **7. Authors contributions**

467 RAZ conceptualized the study. AV and JER contributed to the conception and design of the  
468 study. AV and JER performed experiments and data analysis. RAZ wrote the manuscript and  
469 all authors contributed to the article and approved the submitted version.

470

471 **8. Competing interest statement**

472 The authors declare no competing interest.

473

474 **9. References**

475

476 1. Saei, A. A. *et al.* Comparative Proteomics of Dying and Surviving Cancer Cells  
477 Improves the Identification of Drug Targets and Sheds Light on Cell Life/Death  
478 Decisions. *Mol. Cell. Proteomics* **17**, 1144–1155 (2018).

479 2. Saei, A. A. *et al.* ProTargetMiner as a proteome signature library of anticancer  
480 molecules for functional discovery. *Nat. Commun.* **10**, 5715 (2019).

481 3. Gaetani, M. & Zubarev, R. New Promises of Chemical Proteomics for Drug  
482 Development. *Nov. Approaches Drug Des. Dev.* **2**, 12–14 (2017).

483 4. Moffat, J. G., Vincent, F., Lee, J. A., Eder, J. & Prunotto, M. Opportunities and  
484 challenges in phenotypic drug discovery: an industry perspective. *Nat. Rev. Drug*  
485 *Discov.* **16**, 531–543 (2017).

486 5. Ye, C. *et al.* DRUG-seq for miniaturized high-throughput transcriptome profiling in  
487 drug discovery. *Nat. Commun.* **9**, 4307 (2018).

488 6. Chernobrovkin, A., Marin-Vicente, C., Visa, N. & Zubarev, R. A. Functional  
489 Identification of Target by Expression Proteomics (FITExp) reveals protein targets and  
490 highlights mechanisms of action of small molecule drugs. *Sci. Rep.* **5**, 11176 (2015).

491 7. Hsieh, Y.-C. *et al.* Enhanced Degradation of Dihydrofolate Reductase through  
492 Inhibition of NAD Kinase by Nicotinamide Analogs. *Mol. Pharmacol.* **83**, 339–353  
493 (2013).

494 8. Banerjee, D. *et al.* Novel aspects of resistance to drugs targeted to dihydrofolate  
495 reductase and thymidylate synthase. *Biochim. Biophys. Acta - Mol. Basis Dis.* **1587**,  
496 164–173 (2002).

497 9. Marin-Vicente, C., Lyutvinskiy, Y., Romans Fuertes, P., Zubarev, R. A. & Visa, N.  
498 The Effects of 5-Fluorouracil on the Proteome of Colon Cancer Cells. *J. Proteome Res.*

- 499           **12**, 1969–1979 (2013).
- 500    10.    Ameisen, J. C. On the origin, evolution, and nature of programmed cell death: a  
501            timeline of four billion years. *Cell Death Differ.* **9**, 367–393 (2002).
- 502    11.    Mansilla, S., Llovera, L. & Portugal, J. Chemotherapeutic Targeting of Cell Death  
503            Pathways. *Anticancer. Agents Med. Chem.* **12**, 226–238 (2012).
- 504    12.    Richards, A. L., Merrill, A. E. & Coon, J. J. Proteome sequencing goes deep. *Curr.*  
505            *Opin. Chem. Biol.* **24**, 11–17 (2015).
- 506    13.    Macosko, E. Z. *et al.* Highly Parallel Genome-wide Expression Profiling of Individual  
507            Cells Using Nanoliter Droplets. *Cell* **161**, 1202–1214 (2015).
- 508    14.    Liu, Y., Beyer, A. & Aebersold, R. On the Dependency of Cellular Protein Levels on  
509            mRNA Abundance. *Cell* **165**, 535–550 (2016).
- 510    15.    Bendall, S. C. *et al.* Single-Cell Mass Cytometry of Differential Immune and Drug  
511            Responses Across a Human Hematopoietic Continuum. *Science (80-. ).* **332**, 687–696  
512            (2011).
- 513    16.    Heath, J. R., Ribas, A. & Mischel, P. S. Single-cell analysis tools for drug discovery  
514            and development. *Nat. Rev. Drug Discov.* **15**, 204–216 (2016).
- 515    17.    Zubarev, R. A. The challenge of the proteome dynamic range and its implications for  
516            in-depth proteomics. *Proteomics* **13**, 723–726 (2013).
- 517    18.    Schwanhäusser, B. *et al.* Correction: Corrigendum: Global quantification of  
518            mammalian gene expression control. *Nature* **495**, 126–127 (2013).
- 519    19.    Budnik, B., Levy, E., Harmange, G. & Slavov, N. SCoPE-MS: mass spectrometry of  
520            single mammalian cells quantifies proteome heterogeneity during cell differentiation.  
521            *Genome Biol.* **19**, 161 (2018).
- 522    20.    Emmott, E. *et al.* How to perform quantitative single cell proteomics with SCoPE2. *J.*  
523            *Biomol. Tech.* **31**, S36–S37 (2020).

- 524 21. Specht, H. *et al.* Single-cell proteomic and transcriptomic analysis of macrophage  
525 heterogeneity using SCoPE2. *Genome Biol.* **22**, 50 (2021).
- 526 22. Zhu, Y. *et al.* Nanodroplet processing platform for deep and quantitative proteome  
527 profiling of 10-100 mammalian cells. *Nat. Commun.* **9**, 882 (2018).
- 528 23. Zhang, P. *et al.* Carrier-Assisted Single-Tube Processing Approach for Targeted  
529 Proteomics Analysis of Low Numbers of Mammalian Cells. *Anal. Chem.* **91**, 1441–  
530 1451 (2019).
- 531 24. Tsai, C.-F. *et al.* An Improved Boosting to Amplify Signal with Isobaric Labeling  
532 (iBASIL) Strategy for Precise Quantitative Single-cell Proteomics. *Mol. Cell.*  
533 *Proteomics* **19**, 828–838 (2020).
- 534 25. Cheung, T. K. *et al.* Defining the carrier proteome limit for single-cell proteomics. *Nat.*  
535 *Methods* **18**, 76–83 (2021).
- 536 26. Oh, B. Y. *et al.* Intratumor heterogeneity inferred from targeted deep sequencing as a  
537 prognostic indicator. *Sci. Rep.* **9**, 4542 (2019).
- 538 27. Gaetani, M. *et al.* Proteome Integral Solubility Alteration: A High-Throughput  
539 Proteomics Assay for Target Deconvolution. *J. Proteome Res.* **18**, 4027–4037 (2019).
- 540 28. Deutsch, E. W. *et al.* The ProteomeXchange consortium in 2020: Enabling ‘big data’  
541 approaches in proteomics. *Nucleic Acids Res.* **48**, D1145–D1152 (2020).
- 542 29. Spivak, M., Weston, J., Bottou, L., Käll, L. & Noble, W. S. Improvements to the  
543 Percolator Algorithm for Peptide Identification from Shotgun Proteomics Data Sets. *J.*  
544 *Proteome Res.* **8**, 3737–3745 (2009).
- 545 30. Tyanova, S. *et al.* The Perseus computational platform for comprehensive analysis of  
546 (prote)omics data. *Nat. Methods* **13**, 731–740 (2016).
- 547 31. Yu, S.-H., Kyriakidou, P. & Cox, J. Isobaric Matching between Runs and Novel PSM-  
548 Level Normalization in MaxQuant Strongly Improve Reporter Ion-Based

- 549 Quantification. *J. Proteome Res.* **19**, 3945–3954 (2020).
- 550 32. Leek, J. T., Johnson, W. E., Parker, H. S., Jaffe, A. E. & Storey, J. D. The sva package  
551 for removing batch effects and other unwanted variation in high-throughput  
552 experiments. *Bioinformatics* **28**, 882–883 (2012).
- 553
- 554



555 **10. Figure legends**

556

557 **Figure 1.** SCCP workflow. The workflow developed for SCCP included cell culturing and  
558 treatment with drugs, isolation of individual cells by FACS, protein extraction and digestion,  
559 TMT labeling of thus obtained tryptic peptides followed by multiplexing, LC-MS/MS and  
560 statistical data analysis. All steps are optimized for achieving the desired proteome depth and  
561 quantitative correlation with bulk analysis. In the figure, split carrier proteome occupies two  
562 channels (131N and 131C) in a TMT11plex set, with two other channels (130N and 130C)  
563 remaining empty (dotted lines). Identification of peptides is achieved via matching masses of  
564 sequence-specific fragments, and quantification is performed by the abundances of the low-  
565 mass TMT reporter ions.

566

567 **Figure 2.** Benchmarking SCCP data. A) Correlation between the protein regulations in the  
568 semi-bulk CPs (y-axis) and the median SC data (x-axis). B) Volcano plot of protein regulations  
569 obtained from SCCP data showing MTX target DHFR to be among the most significantly  
570 upregulated proteins. The curved lines separate the areas with significantly regulated proteins.

571

572 **Figure 3.** Time-course results upon treatment with MTX. PCA plots of SCCP data as a time  
573 course demonstrating the emergence of separation between the MTX-treated and untreated  
574 attached cells with incubation time, and the corresponding volcano plots of regulated proteins  
575 showing the emergence of DHFR among the top regulated proteins.

576

577 **Figure 4.** Statistical analysis of single cells treated with MTX. A) OPLS-DA analysis of SCCP  
578 data on median protein abundances in G1 and G2 cell groups from MTX treated cells at  
579 different time points together with bulk CP abundances for the total proteome (1170 proteins)

580 and top 100 most abundant proteins. B) Distribution of the main OPLS-DA coordinates of G1  
581 and G2 groups of MTX-treated attached cells at 12 h and 24 h past treatment for total proteome,  
582 top 400 and top 100 proteins. The x-coordinates were normalized such that the coordinates of  
583 the attached and detached cell bulk-analyzed proteomes after 48 h treatment are +1 and -1,  
584 respectively.

585

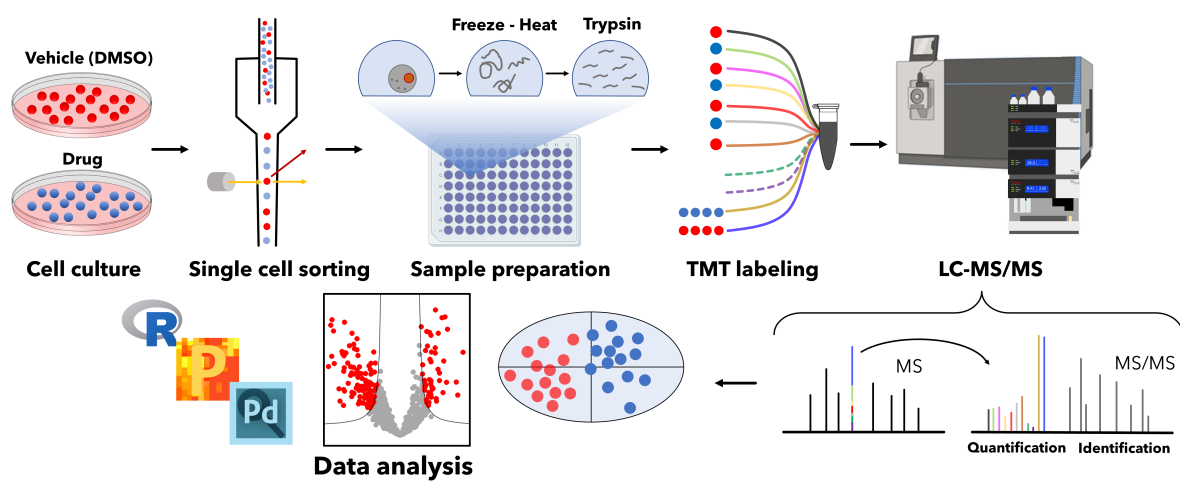
586 **Figure 5.** Time-course results upon treatment with CPT and TDX. PCA plots of SCCP data as  
587 a time course demonstrating the emergence separation between the untreated cells and the  
588 attached cells treated with A) CPT and B) TDX with incubation time, and the corresponding  
589 volcano plots of regulated proteins showing the emergence of the known drug target among the  
590 top regulated proteins.

591

592 **Figures**

593

594



595

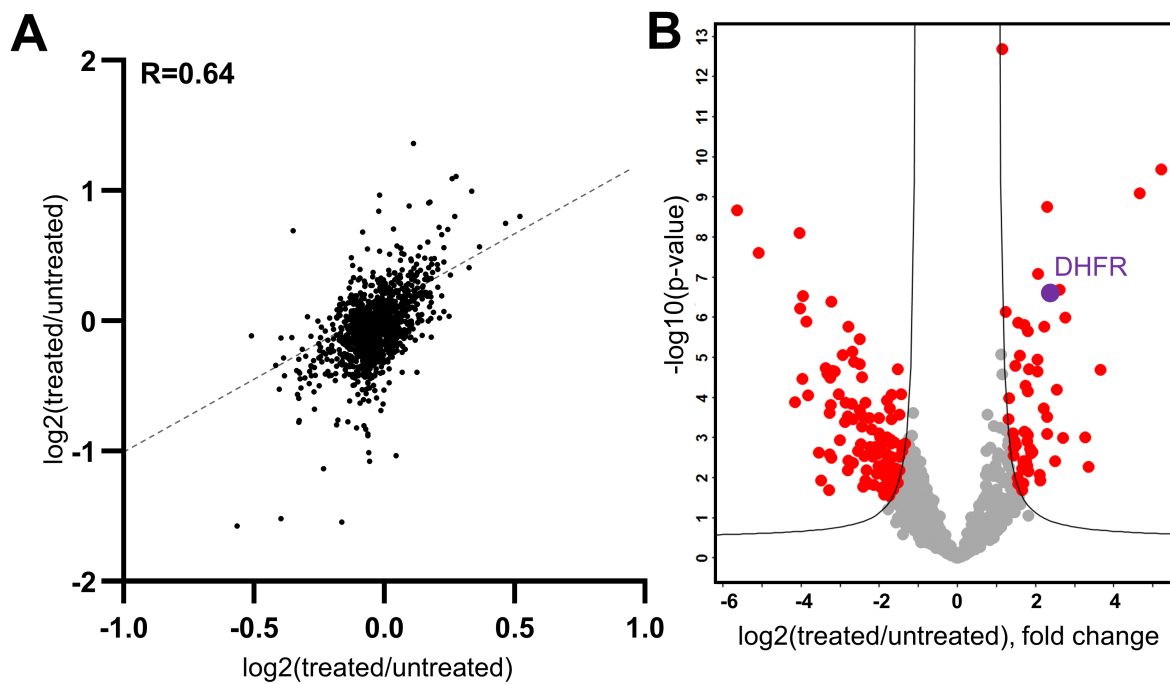
596

597

598

599

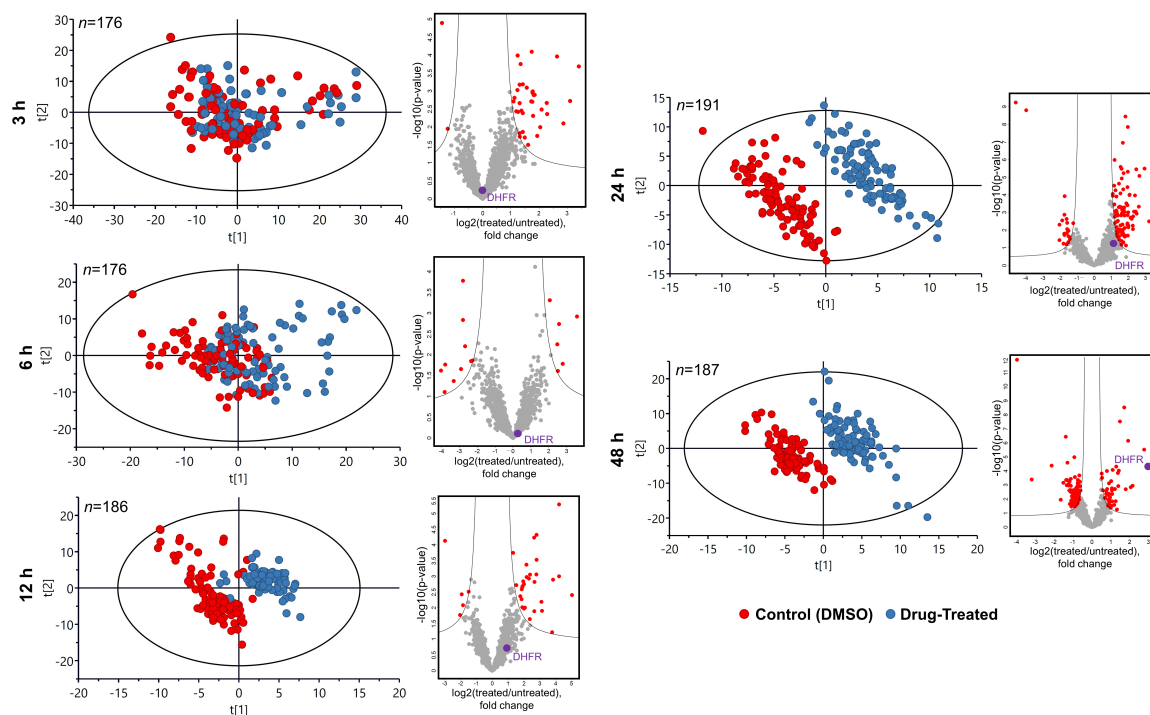
**Figure 1.**



600  
601

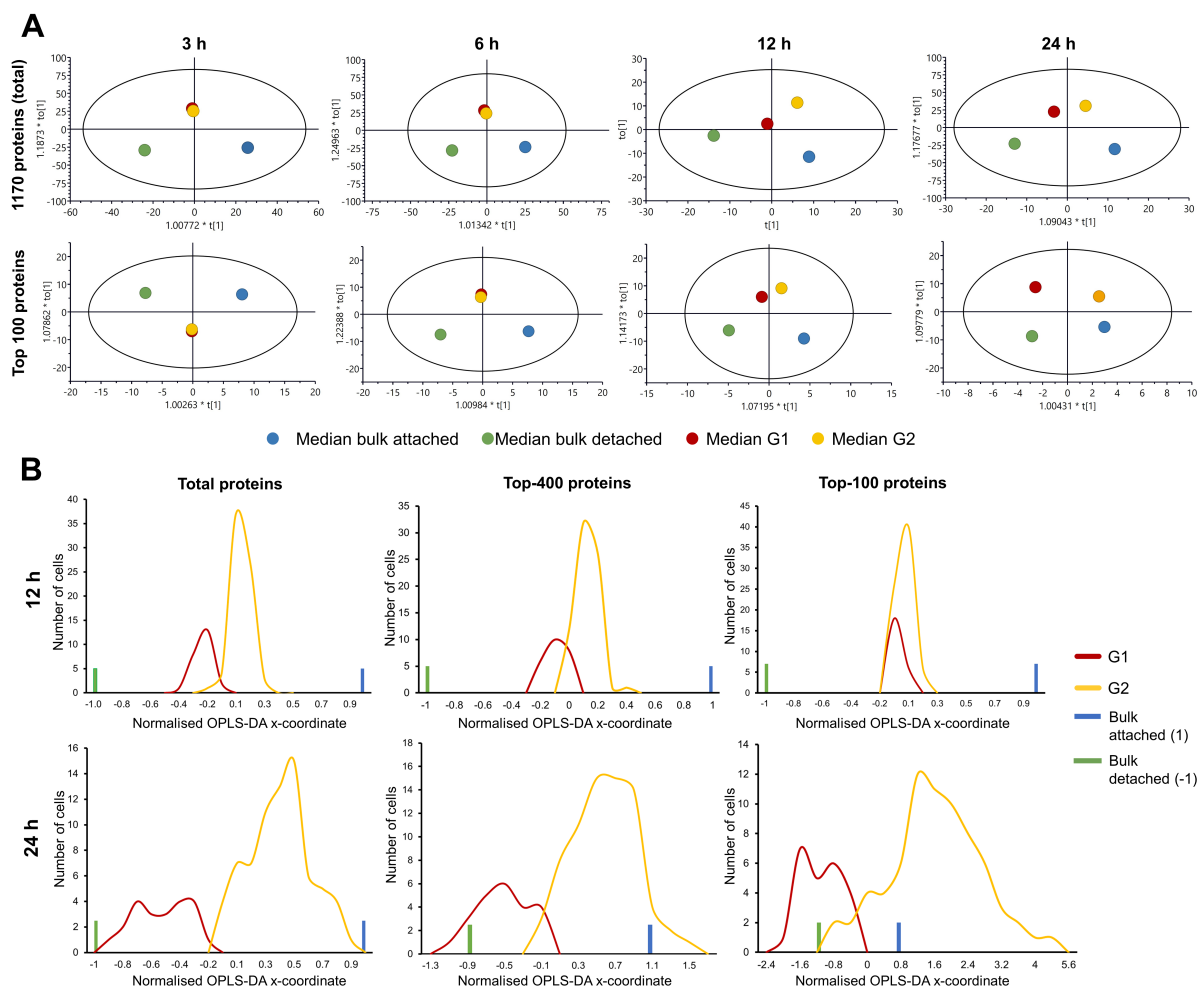
602 **Figure 2.**

603  
604



605  
606  
607  
608

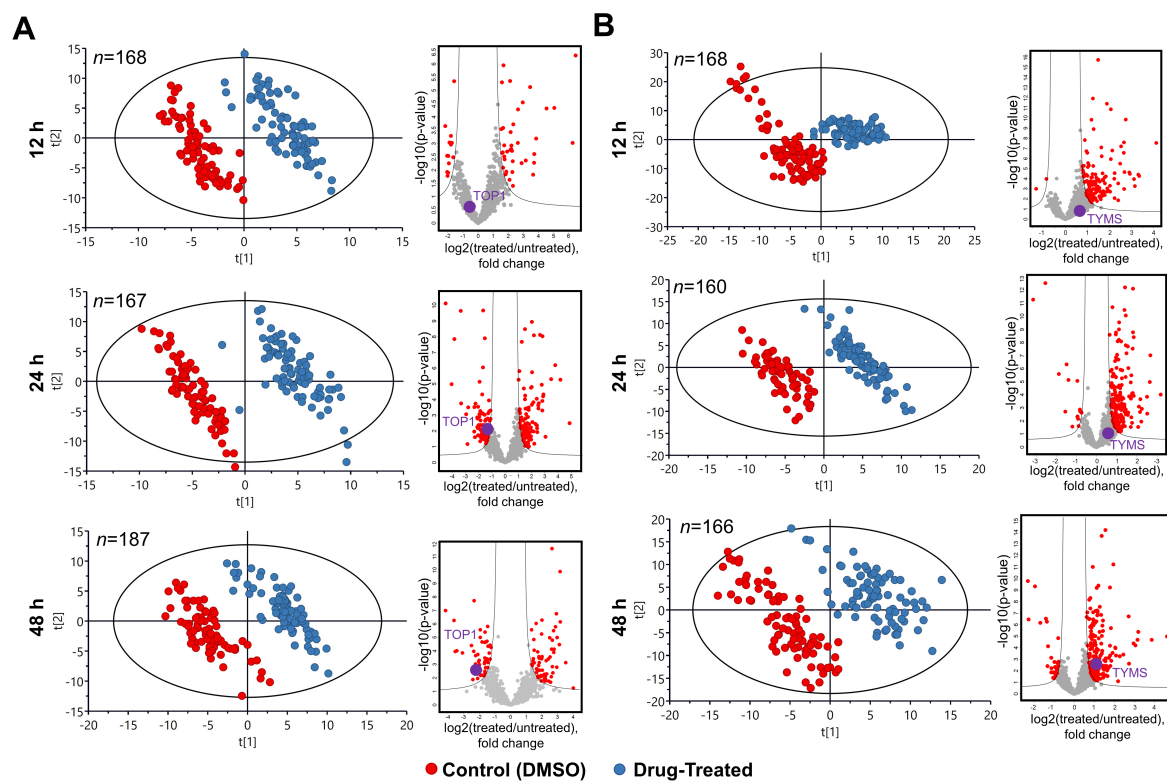
**Figure 3.**



609  
610  
611  
612

**Figure 4.**

613



614  
615

616 **Figure 5.**  
617